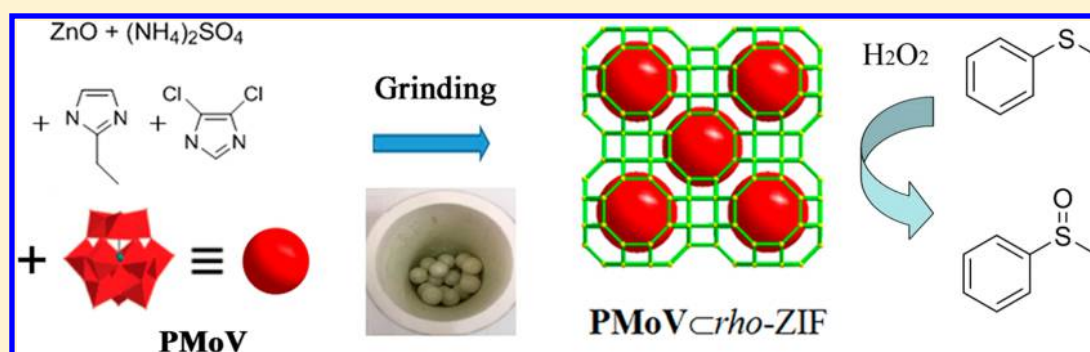


Efficient Mechanochemical Synthesis of Polyoxometalate@ZIF Complexes as Reusable Catalysts for Highly Selective Oxidation

Xiaoxiao Zhao,[†] Yunpeng Duan,[†] Fei Yang,[‡] Wei Wei,^{*,‡} Yanqing Xu,^{*,†} and Changwen Hu[†][†]Key Laboratory of Cluster Science, Ministry of Education of China, Beijing Key Laboratory of Photoelectric/Electrophotonic Conversion Materials, School of Chemistry, Beijing Institute of Technology, Beijing 100081, P. R. China[‡]Department of Chemistry, Capital Normal University, Beijing 100048, P. R. China

S Supporting Information



ABSTRACT: One-pot mechanochemical synthesis was demonstrated to be an efficient strategy to synthesize host–guest POM@rho-ZIF complexes (POM = polyoxometalate; rho-ZIF = zeolitic imidazolate framework with rho topology) with high crystallinity. In this work, the metastable rho-ZIF with large interior cavities and windows was used as host matrix for encapsulating and immobilizing bulky guest molecules with high loading efficiency and chemical stability. As novel catalysts, POM@rho-ZIF complexes were found effective for the selective oxidation of a series of sulfides to sulfoxides. Moreover, the heterogeneity of these composite catalysts was confirmed by leaching tests, and they can be recycled at least four times without significant loss of activity.

■ INTRODUCTION

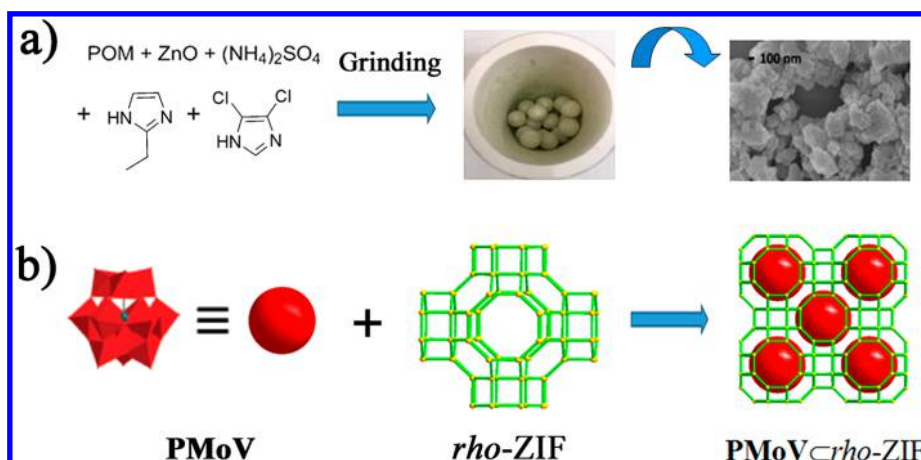
The development of selective and recyclable heterogeneous catalysts is highly desirable yet remains an important challenge. Polyoxometalates (POMs) that possess unique metal–oxygen framework and excellent acid/oxidation catalytic properties have great application prospects in industry.^{1,2} Nevertheless, the application of pure POMs is limited by low surface areas as solid catalysts³ and poor reusability as homogeneous catalysts. To overcome these drawbacks, POMs have been dispersed and immobilized to various supports with high surface areas such as zeolites,⁴ silica,⁵ activated carbon,⁶ mesoporous molecular sieves,⁷ and even metal–organic macrocycles.⁸ Recently, one of the most attractive strategies for heterogenizing POMs is using metal–organic frameworks (MOFs) as host matrix.^{9,10} For instance, Liu¹⁰ and Hill¹¹ et al. have reported a series of highly crystalline Cu-BTC MOFs (BTC = 1,3,5-benzenetricarboxylic acid) incorporating the protonated POMs in hydrothermal synthesis and used them as effective solid catalysts for the hydrolysis and oxidation reactions. However, the solvothermal synthesis to encapsulate POMs into the cages of an MOF in a “ship-in-a-bottle” manner usually suffered from high temperature, long reaction time, a large excess of active POMs centers, bulky organic solvents, and low loading efficiency. In addition, the relatively closed structure and

confined opening of Cu-BTC MOFs hindered the diffusion of bulky substrates to the active sites, limiting the scope of substrate molecules.

Mechanochemical synthesis¹² is emerging as an alternative method for energy-efficiently constructing MOFs, and it avoids bulk solvents, excess reagents, and harsh conditions. Recently, Friščić et al. presented improved approaches including liquid-assisted grinding (LAG) and ion- and liquid-assisted grinding (ILAG) to successfully prepare a number of MOFs.^{13,14} Among these MOFs, zeolitic imidazolate frameworks (ZIFs) are extremely attractive host matrix for synthesizing guest@MOF materials because of the large interior cages and relatively small windows, which are beneficial for encapsulating and immobilizing bulky guest molecules such as POMs. In 2014, Wang et al. has reported that the hydrophilic unsubstituted Keggin-type POMs can be accommodated into the hydrophobic cavities of the in situ formed ZIF-8 with *sod* topology in a mechanochemical process.¹⁵ However, catalysis property of this POM@ZIF material has not been studied, which is probably due to relatively small windows (3.2 Å) and low POM loading (maximal occupancy is ca. 11% of POM in each cavity).

Received: August 26, 2017

Published: November 16, 2017

Scheme 1^a

^a(a) The process of mechanochemical synthesis of PMoVrho-ZIF; the SEM image of PMoVrho-ZIF. (b) The structural representation of PMoVrho-ZIF.

Compared with *sod*-type ZIFs, ZIFs with *rho* topology have larger cavities (18.1 vs 12.5 Å) and windows (7.6 vs 3.2 Å),¹⁶ which can greatly favor the porosity accessibility by bulky substrate molecules and accelerate their diffusion rate. In addition, large interior cavities of *rho*-type ZIFs can increase the POM loading ratio and thus enhance the density of active centers. Consequently, exploiting *rho*-type ZIFs as host matrix for encapsulating POMs to prepare POMrho-ZIF materials as heterogeneous catalysts by the one-pot mechanochemical method is very attractive, not only owing to efficient and environmentally friendly synthesis but also because of the abundant porosity and high chemical stability of the host–guest hybrid materials.

In this work, by one-pot mechanochemical synthesis, metastable *rho*-ZIF was used as host matrix for the first time to efficiently synthesize host–guest complexes PMoVrho-ZIF (PMoV = H₄PMo₁₁VO₄₀, 1; H₅PMo₁₀V₂O₄₀, 2; H₆PMo₉V₃O₄₀, 3) with high crystallinity and chemical stability. In these complexes, POMs were demonstrated to be immobilized within interior cavities of ZIFs with high loading efficiency by physical imprisonment and cannot be released without destroying the host matrix. As novel catalysts, PMoVrho-ZIFs 1–3 were found effective for selective oxidation of a series of sulfides to sulfoxides or sulfones,¹⁷ including bulky diphenyl sulfides. Additionally, the heterogeneity of these composite catalysts was further verified by leaching tests, and they can be recycled at least four times with no significant loss of activity.

RESULTS AND DISCUSSION

Preparation of PMoVrho-ZIF. Because PMoV belongs to the substituted Keggin-type polyoxometalate, the diameter of PMoV is ~10 Å according to the literature,^{15a} which can be readily accommodated in the cavities of *rho*-ZIF (18.1 Å).¹⁶ As shown by Scheme 1, PMoVrho-ZIF complexes were synthesized by an improved ILAG method, which needs only small amounts of salts and liquid to obviously accelerate the formation of MOFs. After a series of comparative experiments, the optimized amounts of 1 mmol of ZnO, 1.5 mmol of 2-ethylimidazole, 1.5 mmol of 4,5-dichloroimidazole, 10 mg of (NH₄)₂SO₄, 200 μL of *N,N*-diethylformamide, and 0.05 mmol of corresponding PMoV were put into the zirconia milling pot and then ball-milled using zirconia balls for 2 × 30 min.

Notably, the formation of *rho*-ZIF is subtle, and overlong grinding time will lead to appearance of impurity with other topologies. After it was washed with a large amount of deionized water and alcohol, the green solids were dried under vacuum and collected to afford complexes 1–3. The PMoV/Zn ratios can be adjusted by altering the initial relative amount of PMoV and ZnO. Nevertheless, the targeted products will not form if the ratio exceeds 1:10. In all cases, almost quantitative samples of 1–3 were obtained.

Characterization of PMoVrho-ZIF. Powder X-ray diffraction (XRD) patterns of complexes 1–3 have typical diffraction peaks that match well with the simulated *rho*-ZIF from the single-crystal XRD data, as shown in Figure 1. It is

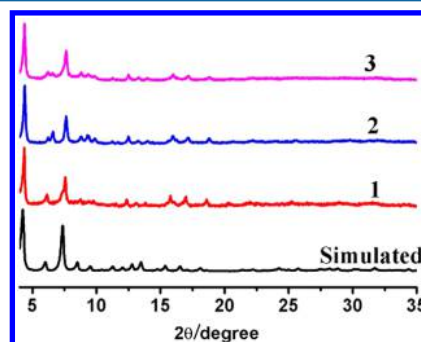


Figure 1. Powder XRD of the simulated *rho*-ZIF, 1, 2, and 3.

noteworthy that the powder XRD patterns of 1–3 are superior to the original ones of *rho*-ZIF reported by Friščić et al.¹² and close to the samples through solution synthesis by Chen et al.^{16a} No diffraction peaks of PMoV were observed in these complexes, which indicated that aggregated PMoV particles were not formed during the mechanochemical synthesis. Therefore, the original ordered structure of *rho*-type ZIF remained intact after encapsulation of PMoV. When the dried samples 1–3 were immersed in various solvents such as water, methanol, ethanol, acetonitrile, and chloroform for 12 h, UV–vis spectra suggested that there were no PMoV leaching out from 1–3 and that all of the complexes kept stable crystallinity in these solvents (Figure S1). Compared with the impurity and easy structural transform of pristine *rho*-ZIF by ILAG method,^{12b} the high chemical stability of PMoVrho-ZIF

materials is probably due to strong POM-ZIF interaction from the complementary shape. Besides, the microscopic architecture morphology and granularity of **1** were studied by scanning electron microscopy (SEM) images, which demonstrated that all composites are exactly nanoparticles from 50 to 400 nm (Figure S2).

The Fourier transform infrared (FT-IR) spectra of **1–3** exhibited that the typical characteristic peaks of **PMoV** (1060, 960, 871, and 784 cm^{-1} , respectively, corresponding to the $\text{P}-\text{O}_a$, $\text{Mo}=\text{O}_d$, $\text{Mo}-\text{O}_b-\text{Mo}$, and $\text{Mo}-\text{O}_c-\text{Mo}$ band vibrations¹⁸) and ρ -ZIF (2971, 1631, 1452, and 1279 cm^{-1}) all existed in **PMoVCrho-ZIF** and proved successful hybridization of **PMoV** and ρ -ZIF (Figure S3–S5).

Furthermore, the components of **PMoVCrho-ZIF** were confirmed by inductively coupled plasma atomic emission spectrometry (ICP-AES). Taking **1** as an example, according to the molar ratio of $\text{Zn}/\text{Mo} = 2.75$, it represented that $\sim 79.4\%$ cavities of ρ -ZIFs are occupied by $\text{H}_4\text{PMo}_{11}\text{VO}_{40}$. The ICP-AES results of **2** ($\text{Zn}/\text{Mo} = 2.67$) and **3** ($\text{Zn}/\text{Mo} = 2.81$) revealed that the occupancy of **PMoV** in each cavity is 89.9% and 94.9%, respectively.

The N_2 adsorption isotherms of **1–3** were measured at 77 K to evaluate the effects of **PMoV** encapsulation into the large cages of the ρ -ZIF (Figure 2). The Brunauer–Emmett–

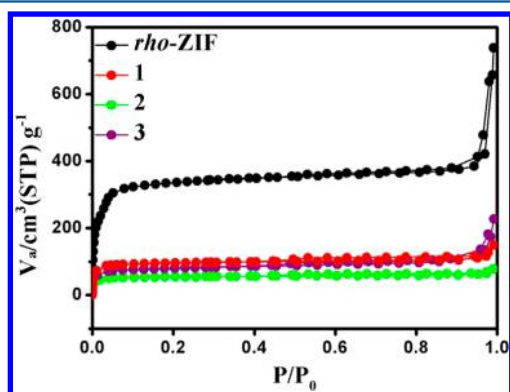


Figure 2. N_2 adsorption–desorption isotherms of pristine ρ -ZIF, **1**, **2**, and **3**.

Teller (BET) surface areas of pristine ρ -ZIF, **1**, **2**, and **3** are 1113, 379, 269, and 318 $\text{m}^2 \text{g}^{-1}$, respectively, which suggest obvious reduction after introducing **PMoV** into the reaction systems. These results indicated that the cages in ρ -ZIF are indeed occupied by **PMoV**.

Catalytic Oxidation. By virtue of the excellent stability in common solvents and highly ordered porosity, **PMoVCrho-ZIF** **1–3** are extraordinarily attractive candidates as heterogeneous catalysts. As we know, vanadium-substituted Keggin-type $\text{PMo}_{12-n}\text{V}_n\text{O}_{40}$ ($n = 1–3$, **PMoV**) have been investigated for effectively catalyzing oxidation reactions;¹⁹ thus, sulfether oxidation with hydrogen peroxide was selected as the model reaction for **PMoVCrho-ZIF** catalysts. In comparison with the homogeneous **PMoV**, the catalytic selectivity for sulfoxides of all **PMoVCrho-ZIF** systems for oxidizing thioanisoles were significantly enhanced from 51%–85% to 93%–96% (Table 1). Besides, controlled experiments were also performed for pristine ρ -ZIF and a blank under the same conditions, and only $\sim 22\%$ – 23% of thioanisoles were oxidized, which suggested that **PMoV** played a key role in the catalytic performance of **PMoVCrho-ZIF**.

Table 1. Performance of Various Catalysts

catalyst ^a	conversion (%)	select for sulfoxides (%)	system
$\text{H}_4\text{PMo}_{11}\text{VO}_{40}$	97	85	homo
$\text{H}_3\text{PMo}_{10}\text{V}_2\text{O}_{40}$	97	59	homo
$\text{H}_6\text{PMo}_9\text{V}_3\text{O}_{40}$	96	51	homo
$\text{H}_4\text{PMo}_{11}\text{VO}_{40}/\rho\text{-ZIF}$ (1)	97	96	hetero
$\text{H}_3\text{PMo}_{10}\text{V}_2\text{O}_{40}/\rho\text{-ZIF}$ (2)	98	97	hetero
$\text{H}_6\text{PMo}_9\text{V}_3\text{O}_{40}/\rho\text{-ZIF}$ (3)	98	93	hetero
blank	22	95	
ρ -ZIF	22	96	hetero

^aReaction conditions: 0.25 mmol thioanisole, 0.000 45 mmol catalysis, 0.3 mmol H_2O_2 , 25 $^\circ\text{C}$, 2 mL of methanol.

To investigate the heterogeneity of **PMoVCrho-ZIF** catalysts, the reaction activity of the supernatant solution after filtration of the catalyst was studied when the reaction was performed for 30 min. The reaction does not proceed after the removal of **1**, implying no leaching of **PMoV** in the reaction process (Figure 3). More importantly, ICP-AES analysis of the filtrate

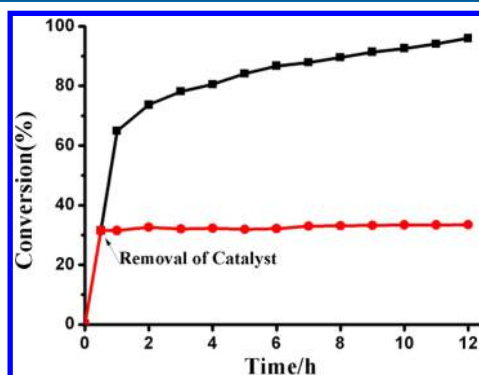


Figure 3. Kinetic plot for the heterogeneity test of catalyst **1**. Reaction conditions: 0.25 mmol of thioanisole; 1.2 mmol of H_2O_2 ; 0.000 45 mmol of **1**; 2 mL of MeOH; 25 $^\circ\text{C}$. The catalyst was removed from the reaction mixture after 30 min.

demonstrated that there are only traces of Mo (16 ppm), and no other metals were detected in the supernatant solution. Consistent with ICP-AES results, the UV–vis spectroscopy further confirmed that no **PMoV** were existing in the filtrate (Figure S6).

Because of the exceptional catalytic activity in the oxidation of thioanisoles, **1** was chosen as the model catalyst to optimize the reaction conditions, and the selected examples are summarized in Table 2. Several reaction variables such as the solvent, oxidant amount, reaction time, and catalyst amount were modulated to afford optimized conditions, which representatively involved 0.25 mmol of thioanisole, 0.3 mmol of H_2O_2 , 0.00045 mmol of catalyst, and 2 mL of methanol at 25 $^\circ\text{C}$ for 12 h.

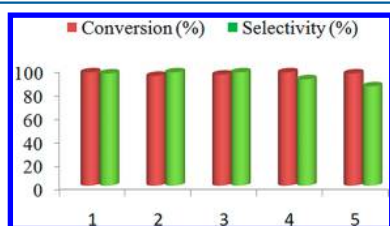
To evaluate the recyclability of catalyst **1**, the catalyst was isolated by sedimentation after each experiment and then washed with EtOH and H_2O and dried under vacuum for using

Table 2. Effect of Reaction Conditions^a for the Oxidation of Thioanisole with H₂O₂

entry	solvent	oxygenant (mmol)	time (h)	conversion (%)	select for sulfoxides (%)
1	MeCN	0.55	18	99	4
2	EtOH	0.55	18	99	73
3	BDO	0.55	18	99	19
4	CHCl ₃	0.55	18	99	42
5	MeOH	0.55	18	99	79
6	MeCN	0.55	18	>99	<1
7	MeCN	0.3	18	90	70
8	MeOH	0.3	18	>99	>99
9	MeOH	0.3	8	88	>99
10	MeOH	0.3	12	99	>99

^aReaction conditions: 0.25 mmol of thioanisole, 0.00045 mmol of catalyst, H₂O₂ (30%), 25 °C, 2 mL of solvent. BDO is 1,4-butylene glycol.

in the subsequent run. As shown by Figure 4, the catalyst can be reusable with no evident loss of activity in oxidation for at

**Figure 4.** Recyclability of catalyst in the selective oxidation of thioanisole.

least four times, and FT-IR spectra and powder XRD of catalysts showed no obvious alteration after five cycles (Figures S7 and S8). The excellent activity and selectivity for the transformation of thioanisoles to sulfoxides of the catalyst encouraged us to explore the selective oxidation of other sulfether compounds. With optimized conditions in hand, we explored the scope of substrates with a series of valuable sulfether compounds. As shown in Table 3, it is reasonable to conclude that as the size of the substrates increase, the conversion and selectivity of substrates decrease slightly owing to the larger steric hindrance. However, the activity and selective oxidation of various sulfides retained high catalytic level.

CONCLUSION

In summary, one-pot mechanochemical synthesis has been demonstrated to be an efficient and environmentally friendly method to prepare host–guest POMCMOF complexes with high crystallinity, and vanadium-substituted Keggin-type POMs can be accommodated within the cavities of *rho*-type ZIF with high loading efficiency and chemical stability by physical imprisonment and cannot be released without destroying the host matrix. To our knowledge, this is the first example that metastable *rho*-ZIF with large interior cavities and windows is used as host matrix for encapsulating and immobilizing bulky guest molecules. More importantly, the mechanochemically prepared POMCMOF materials were used as effective heterogeneous catalyst for selective oxidation of a series of sulfides to sulfoxides and can be recycled at least four times without significant loss of activity. This work provides a versatile and efficient strategy for design and synthesis of novel catalysis systems that realize excellent dispersion and immobilization of the catalytically active centers. Further

Table 3. Substrate Expansion for Catalytic Oxidation^a of Thioether by 1

Entry	Substrate	Conversion (%)	Selection for sulfoxides (%)
1		97.0	95.5
2		92.8	84.2
3		90.4	89.5
4		94.4	91.3
5		82.7	89.0
6		97.1	92.0
7		>99	91.3

^aReaction conditions: 0.25 mmol of substrates, 0.000 45 mmol of catalyst, 0.3 mmol of H₂O₂, 25 °C, 2 mL of MeOH.

attempts to encapsulate various guest molecules for extending the functionality of MOFs are being undertaken.

EXPERIMENTAL SECTION

Materials and Methods. All materials used in this work were purchased from commercial sources and used without further purification. **PMoV** ($\text{PMo}_{12-n}\text{V}_n$, $n = 1-3$) were produced according to a procedure described in the literature.^{18a} Powder XRD was performed on a Bruker Focus D8 diffractometer with a $\text{Cu K}\alpha$ X-ray radiation source ($\lambda = 0.154\,056\text{ nm}$). FT-IR spectra were recorded from KBr pellets in the range of $4000-500\text{ cm}^{-1}$ on a Nicolet 170 SXFT-IR spectrometer. Gas chromatography (GC) analyses were performed on a Shimadzu GC-2014C with a flame ionization detector (FID) equipped with an HP-5 ms capillary column in flowing N_2 with a heating rate of $5\text{ }^\circ\text{C min}^{-1}$. GC mass spectra were recorded on an Agilent 7890A-5975C at an ionization voltage of 1200 V . C, H, and N elemental analyses were conducted on a PerkinElmer 240 $^\circ\text{C}$ elemental analyzer, and Mo, W, and V elemental analyses were performed on an axial view ICP-AES. The one-pot mechanochemical synthesis was performed in a ball mill (QM-3C, Nanjing University Instrument Factory, China).

PMoVCrho-ZIF. Synthetic reactions were performed in an 80 mL zirconia milling pot with 10 mm diameter zirconia balls. One millimole of ZnO , 10 mg of $(\text{NH}_4)_2\text{SO}_4$, 1.5 mmol of 2-ethylimidazole (HETIm), 1.5 mmol of 4,5-dichloroimidazole, and 0.05 mmol of corresponding **PMoV** were put into the pot with adding 200 μL of DEF, then the mixture was ground for $2 \times 30\text{ min}$ at 50 Hz. The collected green solids were washed with substantial deionized water and alcohol to eliminate the excess POMs and then dried under vacuum at $80\text{ }^\circ\text{C}$ for 12 h.

General Procedure for Oxidation of Sulfides by H_2O_2 . Sulfides (0.25 mmol), 30% H_2O_2 (0.3 mmol, 33.8 mg), **PMoVCrho-ZIF** (0.00045 mmol), and 2 mL of MeOH were added to a glass tube; then the catalytic reaction proceeded on a Wattecs parallel reactor at $25\text{ }^\circ\text{C}$ for 12 h. After the reaction was completed, the resulting mixture was analyzed by GC-MS and GC.

ASSOCIATED CONTENT

Supporting Information

The Supporting Information is available free of charge on the ACS Publications website at DOI: 10.1021/acs.inorgchem.7b02163.

X-ray powder diffraction patterns, SEM pictures, infrared and UV-vis spectra. (PDF)

AUTHOR INFORMATION

Corresponding Authors

*E-mail: wwei@cnu.edu.cn. (W.W.)

*E-mail: xyq@bit.edu.cn. (Y.-Z.X.)

ORCID

Wei Wei: 0000-0002-8123-1374

Yanqing Xu: 0000-0002-8310-1944

Changwen Hu: 0000-0002-9026-1145

Author Contributions

All authors have given approval to the final version of the manuscript.

Notes

The authors declare no competing financial interest.

ACKNOWLEDGMENTS

This study was supported by the National Natural Science Foundation of China (Project Nos. 21271025, 11474204, and 21202007) and the Research Foundation of Beijing Institute of Technology (No. 20151942007).

REFERENCES

- (a) Long, J. R.; Yaghi, O. M. The pervasive chemistry of metal-organic frameworks. *Chem. Soc. Rev.* **2009**, *38*, 1213-1214. (b) Férey, G. Hybrid porous solids: past, present, future. *Chem. Soc. Rev.* **2008**, *37*, 191-214. (c) Kitagawa, S.; Kitaura, R.; Noro, S. Functional porous coordination polymers. *Angew. Chem., Int. Ed.* **2004**, *43*, 2334-2375.
- (a) Dolbecq, A.; Dumas, E.; Mayer, C. R.; Mialane, P. Hybrid organic-inorganic polyoxometalate compounds: from structural diversity to applications. *Chem. Rev.* **2010**, *110*, 6009-6048. (b) Adam, W.; Herold, M.; Hill, C. L.; Saha-Moller, C. R. Allylic CH oxidation versus epoxidation of 2-cyclohexenols, catalyzed by chromium- and manganese-substituted polyoxometalates and salen complexes. *Eur. J. Org. Chem.* **2002**, *2002*, 941-946. (c) Kozhevnikov, I. V. For recent reviews see *Chem. Rev.* **1987**, *56*, 811-825. (d) Misono, M. Heterogeneous catalysis by heteropoly compounds of molybdenum and tungsten. *Catal. Rev.: Sci. Eng.* **1987**, *29*, 269-321. (e) Misono, M. Errata and Addenda. *Catal. Rev.: Sci. Eng.* **1988**, *30*, 339-340.
- Du, D. Y.; Qin, J. S.; Li, S. L.; Su, Z. M.; Lan, Y. Q. Recent advances in porous polyoxometalate-based metal-organic framework materials. *Chem. Soc. Rev.* **2014**, *43*, 4615-4632.
- (a) Savelieva, G. A.; Abdulkalykov, D. B.; Dossunov, K. Research of the activity of catalysts on the base of $\text{H}_3\text{PW}_{12}\text{O}_{40}$ in partial oxidative conversion of $\text{C}_3\text{-C}_4$ alkanes. *Catal. Lett.* **2009**, *128*, 106-110.
- (a) Lefebvre, F. ^{31}P MAS NMR study of $\text{H}_3\text{PW}_{12}\text{O}_{40}$ supported on silica: formation of $(\equiv\text{SiOH}_2^+)(\text{H}_3\text{PW}_{12}\text{O}_{40}^-)$. *J. Chem. Soc., Chem. Commun.* **1992**, 756-757. (b) Kozhevnikov, I. V.; Kloetstra, K. R.; Sinnema, A.; Zandbergen, H. W.; van Bekkum, H. van. Study of catalysts comprising heteropoly acid $\text{H}_3\text{PW}_{12}\text{O}_{40}$ supported on MCM-41 molecular sieve and amorphous silica. *J. Mol. Catal. A: Chem.* **1996**, *114*, 287-298. (c) Guo, Y. H.; Wang, Y. H.; Hu, C. W.; Wang, Y. H.; Wang, E. B.; et al. Microporous polyoxometalates POMs/ SiO_2 : synthesis and photocatalytic degradation of aqueous organochlorine pesticides. *Chem. Mater.* **2000**, *12*, 3501-3508. (d) Peng, G.; Wang, Y. H.; Hu, C. W.; Wang, E. B.; Feng, S. H.; Zhou, Y. C.; Ding, H.; Liu, Y. Y. Heteropolyoxometalates which are included in microporous silica, $\text{Cs}_x\text{H}_{3-x}\text{PMo}_{12}\text{O}_{40}/\text{SiO}_2$ and $\text{Cs}_y\text{H}_{5-y}\text{PMo}_{10}\text{V}_2\text{O}_{40}/\text{SiO}_2$, as insoluble solid bifunctional catalysts: synthesis and selective oxidation of benzyl alcohol in liquid-solid systems. *Appl. Catal., A* **2001**, *218*, 91-99. (e) Guo, Y. H.; Hu, C. W. Heterogeneous photocatalysis by solid polyoxometalates. *J. Mol. Catal. A: Chem.* **2007**, *262*, 136-148.
- (a) Gall, R. D.; Hill, C. L.; Walker, J. E. Carbon powder and fiber-supported polyoxometalate catalytic materials, preparation, characterization, and catalytic oxidation of dialkyl sulfides as mustard (HD) analogues. *Chem. Mater.* **1996**, *8*, 2523-2527. (b) Watson, B. A.; Barteau, M. A.; Haggerty, L.; Lenhoff, A. M.; Weber, R. S. Scanning tunneling microscopy and tunneling spectroscopy of ordered hetero- and isopolyanion arrays on graphite. *Langmuir* **1992**, *8*, 1145-1148.
- (a) Nehate, M.; Bokade, V. V. Selective N-alkylation of aniline with methanol over a heteropolyacid on montmorillonite K10. *Appl. Clay Sci.* **2009**, *44*, 255-258. (b) Jin, H. X.; Wu, Q. Y.; Zhang, P.; Pang, W. Q. Assembling of tungstovanadogermanic heteropoly acid into mesoporous molecular sieve SBA-15. *Solid State Sci.* **2005**, *7*, 333-337. (c) Tarlani, A.; Abedini, M.; Nemati, A.; Khabaz, M.; Amini, M. M. Immobilization of keggins and preysler tungsten heteropolyacids on various functionalized silica. *J. Colloid Interface Sci.* **2006**, *303*, 32-38. (d) Udayakumar, S.; Ajaikumar, S.; Pandurangan, A. A protocol on yields to synthesize commercial imperative bisphenols using HPA and supported HPA: effective condensation over solid acid catalysts. *Appl. Catal., A* **2006**, *302*, 86-95. (e) Karthikeyan, G.; Pandurangan, A. Heteropolyacid ($\text{H}_3\text{PW}_{12}\text{O}_{40}$) supported MCM-41: an efficient solid acid catalyst for the green synthesis of xanthenedione derivatives. *J. Mol. Catal. A: Chem.* **2009**, *311*, 36-45. (f) El Ali, B.; Tijani, J.; Fettouhi, M. Rh(I) or Rh(III) supported on MCM-41-catalyzed selective hydroformylation-acetalization of aryl alkenes: effect of the additives. *Appl. Catal., A* **2006**, *303*, 213-220. (g) Zhu, Z. R.; Yang, W. M. Preparation, characterization and shape-selective catalysis of supported heteropolyacid salts $\text{K}_{2.5}\text{H}_{0.5}\text{PW}_{12}\text{O}_{40}$.

(NH₄)_{2.5}H_{0.5}PW₁₂O₄₀ and Ce_{0.83}H_{0.5}PW₁₂O₄₀ on MCM-41 mesoporous silica. *J. Phys. Chem. C* **2009**, *113*, 17025–17031. (h) Liu, Y.; Xu, L.; Xu, B. B.; Li, Z. K.; Jia, L. P.; Guo, W. H. Toluene alkylation with 1-octene over supported heteropoly acids on MCM-41 catalysts. *J. Mol. Catal. A: Chem.* **2009**, *297*, 86–92.

(8) Duan, Y. P.; Wei, W.; Xiao, F.; Xi, Y. R.; Chen, S. L.; Wang, J. L.; Xu, Y. Q.; Hu, C. W. High-valent cationic metal–organic macrocycles as novel supports for immobilization and enhancement of activity of polyoxometalate catalysts. *Catal. Sci. Technol.* **2016**, *6*, 8540–8547.

(9) (a) Du, D. Y.; Qin, J. S.; Li, S. L.; Su, Z. M.; Lan, Y. Q. Recent advances in porous polyoxometalate-based metal–organic framework materials. *Chem. Soc. Rev.* **2014**, *43*, 4615–4632. (b) Han, Q. X.; Qi, B. W.; Ren, M.; He, C.; Niu, J. Y.; Duan, C. Y. Polyoxometalate-based homochiral metal–organic frameworks for tandem asymmetric transformation of cyclic carbonates from olefins. *Nat. Commun.* **2015**, *6*, 10007. (c) Zhang, Z. M.; Zhang, T.; Wang, C.; Lin, Z. K.; Long, L. S.; Lin, W. B. Photosensitizing metal–organic framework enabling visible-light-driven proton reduction by a wells–dawson-type polyoxometalate. *J. Am. Chem. Soc.* **2015**, *137*, 3197–3200. (d) Song, J.; Luo, Z.; Britt, D. K.; Furukawa, H.; Yaghi, O. M.; Hardcastle, K. I.; Hill, C. L. A multiunit catalyst with synergistic stability and reactivity: a polyoxometalate–metal organic framework for aerobic decontamination. *J. Am. Chem. Soc.* **2011**, *133*, 16839–16846. (e) Han, Q. X.; He, C.; Zhao, M.; Qi, B.; Niu, J. Y.; Duan, C. Y. Engineering chiral polyoxometalate hybrid metal–organic frameworks for asymmetric dihydroxylation of olefins. *J. Am. Chem. Soc.* **2013**, *135*, 10186–10189. (f) Canioni, R.; RochMarchal, C.; Sécheresse, F.; Horcajada, P.; Serre, C.; HardiDan, M.; Férey, G.; Grenèche, J. M.; Lefebvre, F.; Chang, J. S.; Hwang, Y. K.; Lebedev, O.; Turner, S.; Van Tendeloo, G. Van. Stable polyoxometalate insertion within the mesoporous metal organic framework MIL-100(Fe). *J. Mater. Chem.* **2011**, *21*, 1226–1233.

(10) (a) Sun, C. Y.; Liu, S. X.; Liang, D. D.; Shao, K. Z.; Ren, Y. H.; Su, Z. M. Highly stable crystalline catalysts based on a microporous metal–organic framework and polyoxometalates. *J. Am. Chem. Soc.* **2009**, *131*, 1883–1888. (b) Ma, F. J.; Liu, S. X.; Sun, C. Y.; Liang, D. D.; Ren, G. J.; Wei, F.; Chen, Y. G.; Su, Z. M. A sodalite-type porous metal–organic framework with polyoxometalate templates: adsorption and decomposition of dimethyl methylphosphonate. *J. Am. Chem. Soc.* **2011**, *133*, 4178–4181. (c) Liu, Y. W.; Liu, S. X.; He, D. F.; Li, N.; Ji, Y. J.; Zheng, Z. P.; Luo, F.; Liu, S. X.; Shi, Z.; Hu, C. W. Crystal facets make a profound difference in polyoxometalate-containing metal–organic frameworks as catalysts for biodiesel production. *J. Am. Chem. Soc.* **2015**, *137*, 12697–12703.

(11) Song, J.; Luo, Z.; Britt, D. K.; Furukawa, H.; Yaghi, O. M.; Hardcastle, K. I.; Hill, C. L. A multiunit catalyst with synergistic stability and reactivity: a polyoxometalate–metal organic framework for aerobic decontamination. *J. Am. Chem. Soc.* **2011**, *133*, 16839–16846.

(12) (a) James, S. L.; Adams, C. J.; Bolm, C.; Braga, D.; Collier, P.; Friščić, T.; Grepioni, F. K.; Harris, D. M.; Hyett, G.; Jones, W.; Krebs, A.; Mack, J.; Maini, L.; Orpen, A. G.; Parkin, I. P.; Shearouse, W. C.; Steed, J. W.; Waddell, D. C. Mechanochemistry: opportunities for new and cleaner synthesis. *Chem. Soc. Rev.* **2012**, *41*, 413–447. (b) Beldon, P. J.; Fábán, L.; Stein, R. S.; Thirumurugan, A.; Cheetham, A. K.; Friščić, T. Rapid room-temperature synthesis of zeolitic imidazolate frameworks by using mechanochemistry. *Angew. Chem., Int. Ed.* **2010**, *49*, 9640–9643. (c) Lazuen-Garay, A.; Pichon, A.; James, S. L. Solvent-free synthesis of metal complexes. *Chem. Soc. Rev.* **2007**, *36*, 846–855. (d) Adams, C. J.; Colquhoun, H. M.; Crawford, P. C.; Lusi, M.; Orpen, G. A. Solid-state interconversions of coordination networks and hydrogen-bonded salts. *Angew. Chem., Int. Ed.* **2007**, *46*, 1124–1128. (e) Yoshida, J.; Nishikiori, S. I.; Kuroda, R. Formation of 1 and 3 D coordination polymers in the solid state induced by mechanochemical and annealing treatments: bis(3-cyano-pentane-2,4-dionato) metal complexes. *Chem. - Eur. J.* **2008**, *14*, 10570–10578. (f) Belcher, W. J.; Longstaff, C. A.; Neckenig, M. R.; Steed, J. W. Channel-containing 1D coordination polymers based on a linear dimetallic spacer. *Chem. Commun.* **2002**, 1602–1603. (g) Braga, D.; Giffreda, S. L.; Grepioni, F.; Pettersen, A.; Maini, L.; Curzi, M.; Polito, M. Mechanochemical

preparation of molecular and supramolecular organometallic materials and coordination networks. *Dalton Trans.* **2006**, 1249–1263.

(13) (a) Friščić, T.; Reid, D. G.; Halasz, I.; Stein, R. S.; Dinnebier, R. E.; Duer, M. J. Ion- and liquid-assisted grinding: improved mechanochemical synthesis of metal–organic frameworks reveals salt inclusion and anion templating. *Angew. Chem.* **2010**, *122*, 724–727. (b) Yuan, W. B.; Friščić, T.; Apperley, D.; James, S. L. High reactivity of metal–organic frameworks under grinding conditions: parallels with organic molecular materials. *Angew. Chem.* **2010**, *122*, 4008–4011. (c) Banerjee, R.; Phan, A.; Wang, B.; Knobler, C.; Furukawa, H.; O’Keeffe, M.; Yaghi, O. M. High-throughput synthesis of zeolitic imidazolate frameworks and application to CO₂ capture. *Science* **2008**, *319*, 939–943. (d) Piloni, M.; Padella, F.; Ennas, G.; Lai, S.; Bellusci, M.; Rombi, E.; Sinig, F.; Pentimalli, M.; Delitala, C.; Scano, A.; Cabras, V.; Ferino, I. Liquid-assisted mechanochemical synthesis of an iron carboxylate metal organic framework and its evaluation in diesel fuel desulfurization. *Microporous Mesoporous Mater.* **2015**, *213*, 14–21. (e) Yang, H.; Orefuwa, S.; Goudy, A. Study of mechanochemical synthesis in the formation of the metal–organic framework Cu₃(BTC)₂ for hydrogen storage. *Microporous Mesoporous Mater.* **2011**, *143*, 37–45. (f) Klimakow, M.; Klobes, P.; Thünemann, A. F.; Rademann, K.; Emmerling, F. Mechanochemical synthesis of metal–organic frameworks: a fast and facile approach toward quantitative yields and high specific surface areas. *Chem. Mater.* **2010**, *22*, 5216–5221. (g) Schlesinger, M.; Schulze, S.; Hietschold, M.; Mehring, M. Evaluation of synthetic methods for microporous metal–organic frameworks exemplified by the competitive formation of [Cu₂(btc)₃(H₂O)₃] and [Cu₂(btc)(OH)(H₂O)]. *Microporous Mesoporous Mater.* **2010**, *132*, 121–127.

(14) (a) Friščić, T.; Fabian, L. Mechanochemical conversion of a metal oxide into coordination polymers and porous frameworks using liquid-assisted grinding (LAG). *CrystEngComm* **2009**, *11*, 743–745. (b) Friščić, T.; Trask, A. V.; Jones, W.; Motherwell, W. D. S. Screening for inclusion compounds and systematic construction of three-component solids by liquid-assisted grinding. *Angew. Chem.* **2006**, *118*, 7708–7712.

(15) (a) Li, R.; Ren, X. Q.; Zhao, J. S.; Feng, X.; Jiang, X.; Fan, X. X.; Lin, Z. G.; Li, X. G.; Hu, C. W.; Wang, B. Polyoxometallates trapped in a zeolitic imidazolate framework leading to high uptake and selectivity of bioactive molecules. *J. Mater. Chem. A* **2014**, *2*, 2168–2173. (b) Li, R.; Ren, X. Q.; Ma, H. W.; Feng, X.; Lin, Z. G.; Li, X. G.; Hu, C. W.; Wang, B. Nickel-substituted zeolitic imidazolate frameworks for time-resolved alcohol sensing and photocatalysis under visible light. *J. Mater. Chem. A* **2014**, *2*, 5724–5729.

(16) (a) He, C. T.; Jiang, L.; Ye, Z. M.; Krishna, R.; Zhong, Z. S.; Liao, P. Q.; Xu, J. Q.; Ouyang, G.; Zhang, J. P.; Chen, X. M. Exceptional hydrophobicity of a large-pore metal–organic zeolite. *J. Am. Chem. Soc.* **2015**, *137*, 7217–7223. (b) Huang, X. C.; Lin, Y. Y.; Zhang, J. P.; Chen, X. M. Ligand-directed strategy for zeolite-type metal–organic frameworks: zinc(II) imidazoles with unusual zeolitic topologies. *Angew. Chem., Int. Ed.* **2006**, *45*, 1557–1559.

(17) (a) Romero, A.; Ramos, E.; Ares, I.; et al. Fipronil sulfone induced higher cytotoxicity than fipronil in SH-SY5Y cells: protection by antioxidants. *Toxicol. Lett.* **2016**, *252*, 42–49. (b) Qi, W.; Wang, Y.; Li, W.; Wu, L. Surfactant-encapsulated polyoxometalates as immobilized supramolecular catalysts for highly efficient and selective oxidation reactions. *Chem. - Eur. J.* **2010**, *16*, 1068–1078. (c) Qu, X.; Guo, Y.; Hu, C. Preparation and heterogeneous photocatalytic activity of mesoporous H₃PW₁₂O₄₀/ZrO₂ composites. *J. Mol. Catal. A: Chem.* **2007**, *262*, 128–135. (d) Wang, F.; Liu, C.; Liu, G.; Li, W. X.; Liu, J. H. Selective oxidation of sulfides to sulfoxides using hydrogen peroxide over Au/CTN–silica catalyst. *Catal. Commun.* **2015**, *72*, 142–146. (e) Frenzel, R.; Sathicq, Á. G.; Blanco, M. N.; Romanelli, G. P.; Pizzio, L. R. Carbon-supported metal-modified lacunary tungstosilicic polyoxometallates used as catalysts in the selective oxidation of sulfides. *J. Mol. Catal. A: Chem.* **2015**, *403*, 27–36.

(18) (a) Tsigdinos, G. A.; Hallada, C. J. Molybdovanadophosphoric acids and their salts. I. investigation of methods of preparation and characterization. *Inorg. Chem.* **1968**, *7*, 437–441. (b) Predoeva, A.;

Damyanova, S.; Gaigneaux, E. M.; et al. The surface and catalytic properties of titania-supported mixed PMoV heteropoly compounds for total oxidation of chlorobenzene. *Appl. Catal., A* **2007**, 319, 14–24.

(19) (a) Yang, H.; Li, J.; Wang, L. Y.; Dai, W.; Lv, Y.; Gao, S. Exceptional activity for direct synthesis of phenol from benzene over PMoV@MOF with O₂. *Catal. Commun.* **2013**, 35, 101–104. (b) Yang, H.; Li, J.; Zhang, H. Y.; Lv, Y.; Gao, S. Facile synthesis of POM@MOF embedded in SBA-15 as a steady catalyst for the hydroxylation of benzene. *Microporous Mesoporous Mater.* **2014**, 195, 87–91. (c) Tong, J. H.; Wang, W. H.; Su, L. D.; Li, Q.; Liu, F. F.; Ma, W. M.; Lei, Z. Q.; Bo, L. L. Highly selective oxidation of cyclohexene to 2-cyclohexene-1-one over polyoxometalate/metal–organic framework hybrids with greatly improved performances. *Catal. Sci. Technol.* **2017**, 7, 222–230.